

# A spectrophotometric study of neodymium(III) complexation in sulfate solutions at elevated temperatures

Art.A. Migdisov<sup>a,\*</sup>, V.V. Reukov<sup>b</sup>, A.E. Williams-Jones<sup>a</sup>

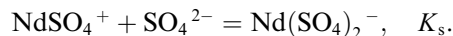
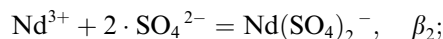
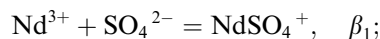
<sup>a</sup> Department of Earth and Planetary Sciences, McGill University, Montréal, Que., Canada H3A 2A7

<sup>b</sup> IREM RAS, Staromonetny per. 35, Moscow 109017, Russian Federation

Received 21 July 2005; accepted in revised form 3 November 2005

## Abstract

The formation constants of neodymium complexes in sulfate solutions have been determined spectrophotometrically at temperatures of 30–250 °C and a pressure of 100 bars. The dominant species in the solution are  $\text{NdSO}_4^+$  and  $\text{Nd}(\text{SO}_4)_2^-$ , with the latter complex being more important at higher temperature. Equilibrium constants were calculated for the following reactions:



The values of  $\beta_1$  and  $\beta_2$ , were determined for 30 and 100 °C, whereas for higher temperatures it was only possible to determine the stepwise formation constant  $K_s$ . The values of the formation constants obtained in this study for 30 and 100 °C are in excellent agreement with those predicted theoretically by Wood [Wood, S.A., 1990b. The aqueous geochemistry of the rare-earth elements and yttrium. 2. Theoretical predictions of speciation in hydrothermal solutions to 350 °C at saturation water vapor pressure. *Chem. Geol.* **88** (1–2), 99–125] and Haas et al. [Haas, J.R., Shock, E.L., Sassani, D.C., 1995. Rare earth elements in hydrothermal systems: estimates of standard partial molal thermodynamic properties of aqueous complexes of the rare earth elements at high pressures and temperatures. *Geochim. Cosmochim. Acta* **59** (21), 4329–4350], and those for the stepwise formation constant ( $K_s$ ) agree reasonably well with the predictions of Wood (1990b).

© 2005 Elsevier Inc. All rights reserved.

## 1. Introduction

During the past fifteen years numerous studies in a variety of geological settings have demonstrated that the Rare Earth elements (REE) are mobilized by hydrothermal fluids (e.g., Buhn and Rankin, 1999; MacLean, 1988; Olivo and Williams-Jones, 1999; Schandl and Gorton, 1991), and in some cases are concentrated to economically appreciable levels by these processes (e.g., Smith and Henderson, 2000; Williams-Jones et al., 2000). However, modelling of

the behavior of REE in hydrothermal solutions has been severely compromised by a lack of experimental data.

Most of the data available on REE speciation at hydrothermal conditions are extrapolations of experimental data obtained at room temperature (Haas et al., 1995; Wood, 1990b). Experimental studies at elevated temperatures have been limited to the complexes of the REE with chloride (Gammons et al., 1996, 2002; Migdisov and Williams-Jones, 2002; Stepanchikova and Kolonin, 1999), hydroxide (Wood et al., 2002), acetate (Wood et al., 2000), and phosphate (Cetiner et al., 2005) ions. However, there are no high temperature experimental data for fluoride, carbonate, or sulfate complexes of REE, which a number of studies have suggested may be the dominant REE species in

\* Corresponding author. Fax: +1 514 398 4680.

E-mail address: [artas@eps.mcgill.ca](mailto:artas@eps.mcgill.ca) (Art.A. Migdisov).

many hydrothermal systems. For example, fluoride complexes are considered to have been responsible for the concentration of REE in the Strange Lake rare metal deposit, Quebec, and the Gallinas Mountain REE-fluoride deposit, New Mexico (Salvi and Williams-Jones, 1990; Williams-Jones et al., 2000). Similarly, sulfate complexes have been invoked to explain the concentrations of REE in anhydrite precipitating seafloor hydrothermal systems (Bach et al., 2003) and some geothermal systems (Lewis et al., 1998). There is thus a pressing need for well constrained high temperature experimental data on the stability of REE complexes with those other ligands. In this study, we report results of an experimental investigation of the speciation of Nd in sulfate-bearing solutions at temperatures up to 250 °C.

## 2. Method

The study was conducted using an in situ, ultraviolet (UV)–visible spectroscopic method similar to that employed in our previous investigation of Nd speciation in Cl-bearing solutions (Migdisov and Williams-Jones, 2002). Experiments were conducted at a temperatures of 30, 100, 150, 200, and 250 °C and a pressure of 100 bars, using a high temperature, flow-through, UV–visible spectroscopic cell. The cell was constructed from grade 4 titanium alloy and was equipped with sapphire windows, which were sealed in the cell using Graflex (polymerized graphite) o-rings. The path length (0.97 cm) was determined by a calibration procedure involving measurements of the absorbance of a solution of Nd (0.28 mol/dm<sup>3</sup>), prepared by dissolution of Nd<sub>2</sub>O<sub>3</sub> (Alfa Aesar, 99.99%) in Nanopure de-ionized water acidified by Optima-grade perchloric acid (Fisher Scientific) to a final pH of 1.56. The spectra for this solution were recorded at 30 °C in a standard 1-cm quartz cuvette and in the experimental flow-through cell. The cell was heated using elements in the cell-body, and temperature was controlled by an Omega CN-2001 regulator to within ±0.5 °C of a pre-determined value. Temperature was measured using a type K thermocouple inserted in a well within the cell. Pressure was controlled using a solution delivery system, consisting of a HP 1050-Ti HPLC pump, PEEK and Ti capillaries, and a PEEK back pressure regulator. Experimental solutions were therefore only in contact with chemically inert materials.

Absorption spectra were collected for 22 to 30 solutions (depending on the isotherm investigated, Table 1), having total Nd concentrations ranging from  $2.0 \times 10^{-2}$  to  $5.7 \times 10^{-2}$  mol/dm<sup>3</sup> (all concentrations here and below are given for solutions at 25 °C), and total sulfate concentrations from  $1 \times 10^{-3}$  to  $4.2 \times 10^{-2}$  mol/dm<sup>3</sup>. The solutions were prepared in three sets with total Nd concentrations of 2, 2.5, and  $5.7 \times 10^{-2}$  mol/dm<sup>3</sup>. This was done by dissolving REacton-grade neodymium(III) oxide (Alfa Aesar, 99.99%) in Nanopure de-ionized water acidified by Optima-grade perchloric acid (Fisher Scientific) to a final pH of 1.56 to prevent hydrolysis of Nd. To compare the experimental molar absorbance of Nd<sup>3+</sup> with that determined during our previous study (using the same system; Migdisov and Williams-Jones, 2002), the first solution of each series was prepared to be sulfate-free. In the remaining solutions, sulfate was introduced by adding corresponding quantities of Na<sub>2</sub>SO<sub>4</sub> (Fisher Scientific, A.C.S.).

The range of concentrations of neodymium and sulfate in the experimental solutions was relatively narrow, because of the following two constraints:

- Nd<sup>3+</sup> has weak molar absorbance (e.g., Migdisov and Williams-Jones, 2002; Stepanchikova and Kolonin, 1999), which decreases with temperature. Thus, to record statistically reliable spectra, we had to use solutions having relatively high total concentrations of Nd ( $>1 \times 10^{-2}$  mol/dm<sup>3</sup>).
- Neodymium sulfate was found to show retrograde solubility with temperature. As a result, precipitation occurred at 150 °C when concentrations of Nd and SO<sub>4</sub><sup>2-</sup> exceeded  $5.7 \times 10^{-2}$  and  $4.4 \times 10^{-2}$ , respectively; at 200 °C when they exceeded  $5.7 \times 10^{-2}$  and  $3.6 \times 10^{-2}$ , respectively; and at 250 °C when they exceeded  $5.7 \times 10^{-2}$  and  $2.8 \times 10^{-2}$ , respectively (concentrations in mol dm<sup>-3</sup>). This caused a systematic shift of recorded spectra to higher values, and led to blockage of capillaries in the solvent delivery system. This behavior was not unexpected, as other sulfates, e.g., anhydrite and celestite are known to display retrograde solubility (Robie and Hemingway, 1995). It was thus necessary to conduct experiments with SO<sub>4</sub><sup>2-</sup> concentrations below these thresholds (and Nd concentrations  $>1 \times 10^{-2}$  mol/dm<sup>3</sup>; constraint a).

Table 1  
Results of the rank analysis of the absorbance matrix

T (°C)	Solutions (number)	ΣNd range (mol/L, 10 <sup>-2</sup> )	ΣSO <sub>4</sub> range (mol/L, 10 <sup>-2</sup> )	Rank of abs. matrix (sulfate free solutions excluded) tolerance			Speciation model
				0.01	0.015	0.02	
30	30	5.7–2.0	4.2–0.1	3	3	3	Nd <sup>3+</sup> +NdSO <sub>4</sub> <sup>+</sup> +Nd(SO <sub>4</sub> ) <sub>2</sub> <sup>-</sup>
100	30	5.7–2.0	4.2–0.1	3	3	3	Nd <sup>3+</sup> +NdSO <sub>4</sub> <sup>+</sup> +Nd(SO <sub>4</sub> ) <sub>2</sub> <sup>-</sup>
150	26	5.7–2.0	3.6–0.1	3	3	2	Nd <sup>3+</sup> + NdSO <sub>4</sub> <sup>+</sup> +Nd(SO <sub>4</sub> ) <sub>2</sub> <sup>-</sup> , and NdSO <sub>4</sub> <sup>+</sup> +Nd(SO <sub>4</sub> ) <sub>2</sub> <sup>-</sup>
200	25	5.7–2.0	3.0–0.1	3	2	2	Nd <sup>3+</sup> +NdSO <sub>4</sub> <sup>+</sup> +Nd(SO <sub>4</sub> ) <sub>2</sub> <sup>-</sup> , and NdSO <sub>4</sub> <sup>+</sup> +Nd(SO <sub>4</sub> ) <sub>2</sub> <sup>-</sup>
250	22	5.7–2.0	2.5–0.1	3	2	2	Nd <sup>3+</sup> + NdSO <sub>4</sub> <sup>+</sup> +Nd(SO <sub>4</sub> ) <sub>2</sub> <sup>-</sup> , and NdSO <sub>4</sub> <sup>+</sup> +Nd(SO <sub>4</sub> ) <sub>2</sub> <sup>-</sup>

Spectrophotometric measurements were made at 0.5-nm intervals over the range 400–900 nm using a Cary 100 double-beam spectrophotometer. To correct the spectra for background absorption, the absorption of the cell filled with Nanopure deionized water was recorded before each of the Nd spectra was collected. To ensure that the recorded spectra represent a state of equilibrium, test spectra were collected for selected solutions at flow rates ranging from 0.05 to 0.3 ml/min, which provided for complete exchange of the solutions in the cell in 20 to 3 min, respectively. No changes in the spectra were detected during these runs, suggesting that equilibrium was established in less than 3 min after the solution entered the heated cell. The total Nd and SO<sub>4</sub> concentrations of the solutions were checked after the runs using neutron activation and HPLC methods (Activation Laboratories, Canada).

An estimate of the error of the measured absorbance values was obtained by repeated measurements (several sets of 5–10 scans at each temperature) of the spectra of a solution having a total Nd concentration of  $2.2 \times 10^{-2}$  mol/dm<sup>3</sup>. It was found that the absorption values were reproducible to a tolerance (uncertainty in absolute units) that varied from 0.01 to 0.02, and that this tolerance increased with increasing temperature and decreasing wavelength.

### 3. Results

The absorption spectra recorded for the sulfate-free solutions were found to be identical to those determined in our previous study (Migdisov and Williams-Jones, 2002). The spectra collected at 30 °C are in good agreement with those of Carnall (1979) and with the electronic spectrum of the hydrated Nd<sup>3+</sup> ion calculated by Kotzian et al. (1995). As can be seen from Fig. 1, heating of the solutions resulted in a significant decrease of the molar absorbance of Nd<sup>3+</sup>, which was calculated from the concentration of Nd<sup>3+</sup> in sulfate-free solutions using the Beer–Lambert law:

$$A = \epsilon_{\text{Nd}^{3+}} \cdot M_{\text{Nd}^{3+}} \cdot l, \quad (1)$$

where  $A$  is absorbance,  $\epsilon$  is the molar absorbance for Nd<sup>3+</sup>,  $l$  is the pathlength, and  $M$  is the molar concentration of Nd<sup>3+</sup> in mol/dm<sup>3</sup>.

Typical spectra for solutions of variable Nd/SO<sub>4</sub><sup>2-</sup> ratio, corrected for solvent and window absorbance, are shown in Figs. 2A and B. The spectra recorded at 30 °C are very similar to those obtained by Lakshman and Buddhu (1982). It can be seen from Fig. 2 that changes in the Nd/SO<sub>4</sub> ratio result in changes to the measured spectra, especially at wavelengths in the range, 560–610 nm. From Fig. 2, it also can be seen that an increase of the concentration of SO<sub>4</sub> relative to Nd results in a red shift of the spectra and an increase in the peak intensities. The effect of temperature is illustrated in Fig. 3. Inspection of this figure indicates that with increasing temperature the spectra also undergo the red shift, but, as was observed for sulfate-free

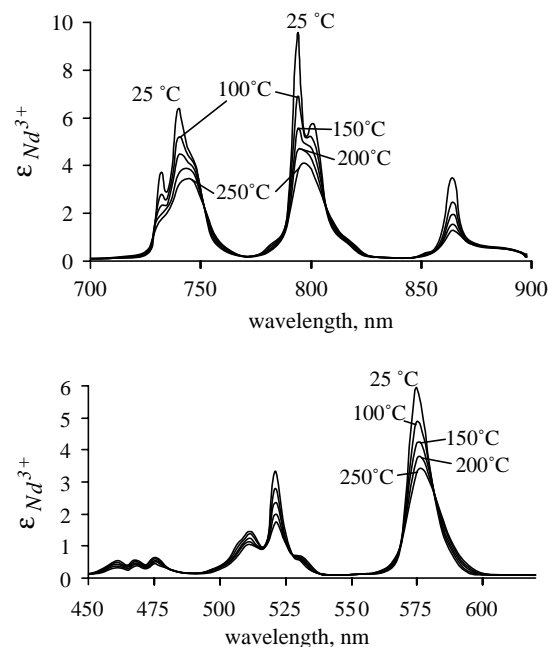


Fig. 1. The molar absorbance of Nd<sup>3+</sup> obtained from spectra for sulfate-free solutions (ClO<sub>4</sub> based).

solutions, peak intensities decrease with temperature. We speculate that the red shift produced by increasing temperature might reflect variations in the stability of Nd(III) sulfate complexes.

### 4. Data treatment

#### 4.1. Speciation model

To develop a chemical model for the solutions investigated, and to determine the number of absorbing Nd(III) species, we used the method of absorbance matrix analysis described by Suleimenov and Seward (2000) and employed previously by us in a study of Nd speciation in chloride-bearing solutions (Migdisov and Williams-Jones, 2002). The reader is referred to these papers for details not covered in the following summary.

In accordance with Beer's law, and assuming a conventional linear model with respect to chemical composition, each of the experimental measurements at any given wavelength is defined by:

$$\frac{A}{l} = \sum_i \epsilon_i \cdot M_i, \quad (2)$$

where  $A$  is absorbance,  $\epsilon_i$  is the molar absorbance of the corresponding species,  $l$  is the pathlength, and  $M_i$  is the molar concentration of the corresponding species. It follows that the number of absorbing species at the temperature investigated is given by the maximum number of linearly independent columns in the rectangular absorbance matrix (solutions/wavelengths). If no two species have the same molar extinction coefficient, this number can be found by determining the rank of the absorbance

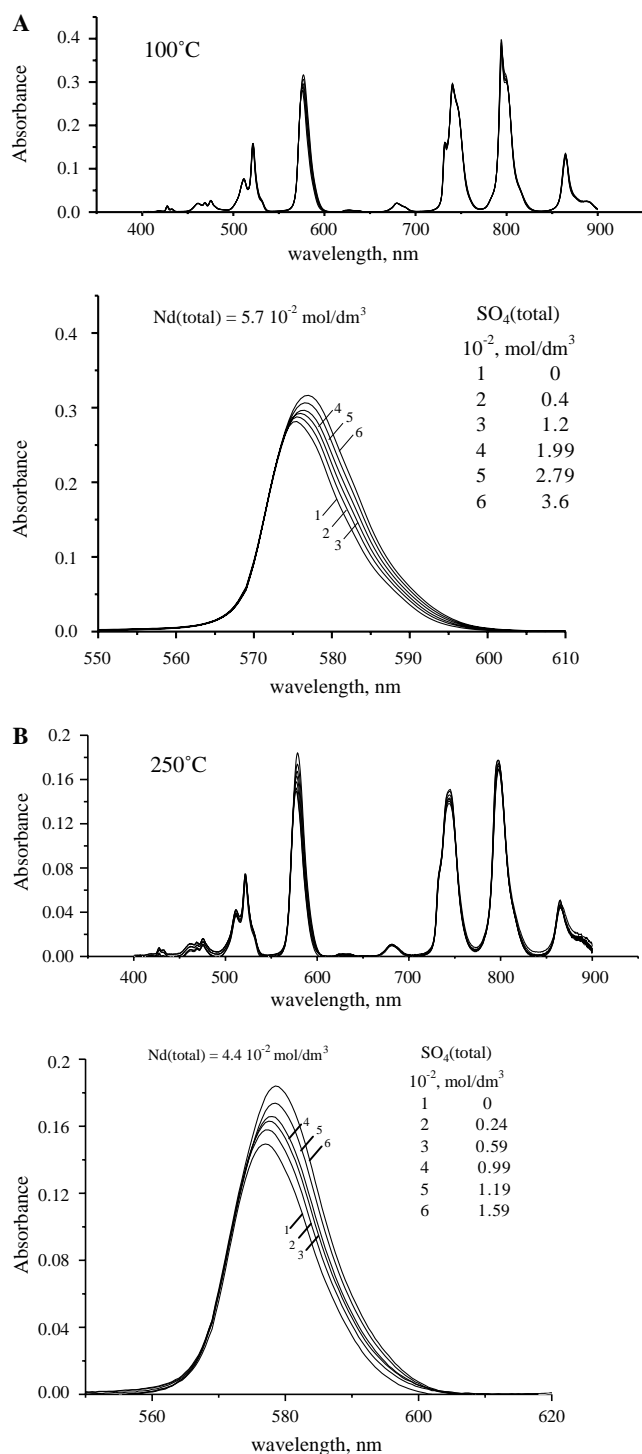


Fig. 2. Examples of isothermal spectra recorded for a set of solutions with different Nd/SO<sub>4</sub> ratios at 100 °C (A) and 250 °C (B).

matrix. The latter was calculated using MATLAB software, which employs a method, based on the singular value decomposition (Dongarra et al., 1979). As the experimentally determined uncertainties in the absorption values varied from 0.010 to 0.020, the results of the rank calculations for these tolerance intervals were taken as the total number of absorbing species. The absorbance matrix was reduced to restrict it to the wavelength ranges for which peaks were

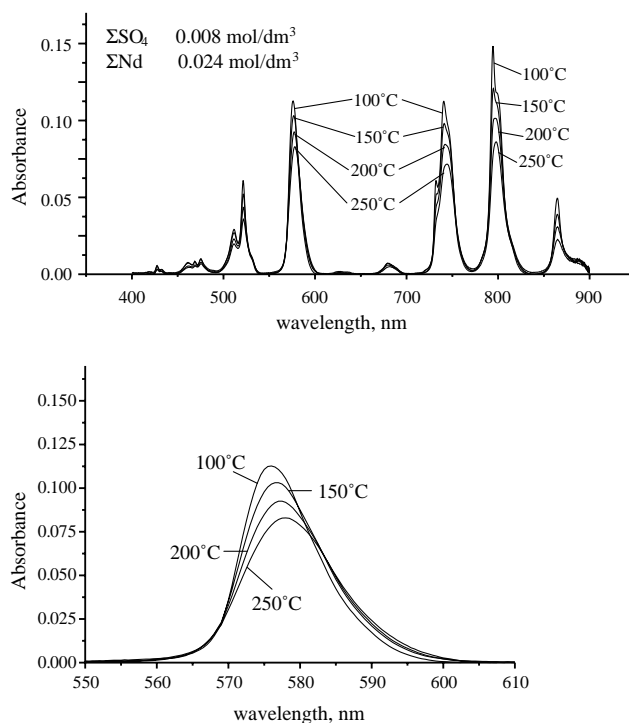


Fig. 3. The effect of temperature on the spectra of neodymium sulfate solutions; peak intensity decreases with increasing temperature.

detected, excluding areas at which maximal absorbance recorded during the runs was below 0.01.

At a tolerance of 0.02, the rank of the reduced absorbance matrix was found to be equal to three for all the temperatures investigated. Moreover, when the sulfate-free solutions (which contain only Nd<sup>3+</sup> among neodymium species) are removed from the absorbance matrix, the rank calculated for 25 and 100 °C remains equal to three, whereas at higher temperatures it decreases to two. This may indicate that, for the range of concentrations tested in the experiments at high temperature, Nd<sup>3+</sup> was present in concentrations insufficient for reliable de-convolution of the absorbance matrix. In those experiments most of the Nd was interpreted to be present as sulfate complexes.

Although all the solutions also contained Na<sup>+</sup>, ClO<sub>4</sub><sup>-</sup>, and SO<sub>4</sub><sup>2-</sup>, these species were omitted as they are transparent in the spectral region investigated. The remainder of the absorbing species were identified based on speciation models published in the literature. Identifying the species for a model involving three absorbing species was straightforward, as the only sulfate complexes described in the literature are NdSO<sub>4</sub><sup>+</sup> and Nd(SO<sub>4</sub>)<sub>2</sub><sup>-</sup> (e.g., Izatt et al., 1969; Wood, 1990a). Thus, for the three-species model we used Nd<sup>3+</sup>, NdSO<sub>4</sub><sup>+</sup>, and Nd(SO<sub>4</sub>)<sub>2</sub><sup>-</sup>, and in the two species model, NdSO<sub>4</sub><sup>+</sup> and Nd(SO<sub>4</sub>)<sub>2</sub><sup>-</sup>.

#### 4.2. Activity model

To estimate activity coefficients of ions of interest, previous experimental studies devoted to REE behavior in aqueous media (e.g., Gammons et al., 1996; Migdisov and

Williams-Jones, 2002; Wood et al., 2000) employed the extended Debye–Hückel equation (Helgeson et al., 1981). Unfortunately, this equation was developed only for the following background electrolytes NaCl, KCl, NaOH, and KOH (Helgeson et al., 1981; Oelkers and Helgeson, 1990; Pokrovskii and Helgeson, 1995, 1997a,b), and was never extended to ClO<sub>4</sub>-dominated solutions. Moreover, comparison of the experimental data with calculations published in the literature (e.g., Weare, 1989) shows that even at relatively modest values of ionic strength (0.2–0.4) this equation fails to accurately predict activities of components of systems containing SO<sub>4</sub><sup>2-</sup> in significant concentrations. Thus, to evaluate activities in the system investigated here, we employed the simplified Pitzer model (Harvie and Weare, 1980; Pitzer and Kim, 1974), which was developed by Millero (1992) for REE in ClO<sub>4</sub>-based solutions. This model uses the truncated form of the Pitzer equation (Harvie and Weare, 1980), and for neodymium sulfate dissolved in a NaClO<sub>4</sub> media gives the following expressions of activity coefficients (for more details see Millero, 1992):

$$\ln \gamma_{\text{Nd}} = z_{\text{Nd}}^2 f^\gamma + 2I(B_{\text{NdClO}_4} + IC_{\text{NdClO}_4}) + I^2(z_{\text{Nd}}^2 B'_{\text{NdClO}_4} + z_{\text{Nd}} C_{\text{NdClO}_4}) \quad (3)$$

$$\ln \gamma_{\text{SO}_4} = z_{\text{SO}_4}^2 f^\gamma + 2I(B_{\text{NaSO}_4} + IC_{\text{NaSO}_4}) + I^2(z_{\text{SO}_4} B'_{\text{NaSO}_4} + z_{\text{SO}_4} C_{\text{NaSO}_4}), \quad (4)$$

where  $I$  is the ionic strength,  $z$  is the charge,  $m$  is the molality of the corresponding ion,  $f^\gamma$  denotes the Debye–Hückel limiting term  $f^\gamma = A^\phi \left[ \frac{\sqrt{I}}{1+1.2\sqrt{I}} + \frac{2}{1.2} \ln(1+1.2\sqrt{I}) \right]$ , and  $A^\phi$  is the Debye–Hückel coefficient. The parameters  $B_{\text{MX}}$ ,  $B'_{\text{MX}}$ , and  $C_{\text{MX}}$  are given by

$$B_{\text{MX}} = \beta_{\text{MX}}^\circ + \frac{\beta_{\text{MX}}^1}{2I} \left( 1 - (1 + 2\sqrt{I}) \exp(-2\sqrt{I}) \right), \quad (5)$$

$$B'_{\text{MX}} = \frac{\beta_{\text{MX}}^1}{2I^2} \left( -1 + (1 + 2\sqrt{I} + 2I) \exp(-2\sqrt{I}) \right), \quad (6)$$

$$C_{\text{MX}} = \frac{C_{\text{MX}}^\phi}{2\sqrt{|z_{\text{M}}z_{\text{X}}|}}, \quad (7)$$

where  $\beta_{\text{MX}}^\circ$ ,  $\beta_{\text{MX}}^1$ , and  $C_{\text{MX}}^\phi$  are the Pitzer ion interaction parameters listed in Table 2, and M and X denote metal and ligand, respectively. As can be seen from Eqs. (3) and (4), ternary interactions and interactions of ions of the same charge (anion–anion, cation–cation) were ignored, due primarily to a lack of data for these parameters. However, given that concentrations of perchlorate in the experimental solutions were at least an order of magnitude greater than those of Nd and SO<sub>4</sub>, and ionic strength never

Table 2  
Pitzer parameters (25 °C) used for the activity coefficient calculations

	$\beta^\circ$	$\beta^1$	$C^\phi$
NaClO <sub>4</sub>	0.0554	0.2755	−0.00118
Na <sub>2</sub> SO <sub>4</sub>	0.01958	1.113	0.0057
Nd(ClO <sub>4</sub> ) <sub>3</sub>	0.754	6.5333	0.00747

Table 3

Temperature derivatives of the Pitzer parameters used for the activity coefficients calculations at  $T > 25$  °C

	$\partial\beta^\circ/\partial T$ (10 <sup>−3</sup> )	$\partial\beta^1/\partial T$ (10 <sup>−3</sup> )	$\partial C^\phi/\partial T$ (10 <sup>−4</sup> )
NaClO <sub>4</sub>	1.296	2.29	−1.62
Na <sub>2</sub> SO <sub>4</sub>	2.36	5.63	−1.72
Nd(ClO <sub>4</sub> ) <sub>3</sub>	1.50	1.50	−1.90

exceeded 0.3, we believe that this approach provides a reasonable approximation of the activity coefficients of the species considered in this study. Temperature derivatives for the ion interaction parameters were taken from Silvester and Pitzer (1978) and Pitzer (1991), and are listed in Table 3.

Following Millero (1992), activity coefficients of sulfate complexes of Nd were calculated using the equation:

$$\ln \gamma_{\text{MX}} = \ln \gamma_{\text{elect}} + 2m_{\text{ClO}_4} B_{\text{MX}}, \quad (8)$$

where

$$\ln \gamma_{\text{elect}} = f^\gamma + 4m_{\text{Na}} m_{\text{ClO}_4} B'_{\text{NaClO}_4} + 2m_{\text{Na}} m_{\text{ClO}_4} C_{\text{NaClO}_4}. \quad (9)$$

The value of  $B_{\text{MX}}$  for NdSO<sub>4</sub><sup>+</sup> was assumed to be equal to the average value of this parameter derived by Millero (1992) for lanthanides (0.62). Owing to a lack of experimental data, we also had to assume that this parameter is temperature independent, and to postulate that  $\gamma_{\text{NdSO}_4^+} = \gamma_{\text{Nd}(\text{SO}_4)_2^-}$ . While the latter assumption is reasonable (many activity models do not distinguish among ions of the same absolute charge), assumption of temperature independence is questionable. However, the assumption of a temperature independence of  $B_{\text{MX}}$  for NdSO<sub>4</sub><sup>+</sup> can be justified by considering the temperature dependence of other REE-bearing components. From Tables 2 and 3 it can be seen that although temperature derivatives of Pitzer parameters for Nd(ClO<sub>4</sub>)<sub>3</sub> are of the same order of magnitude as those for NaClO<sub>4</sub> and Na<sub>2</sub>SO<sub>4</sub>, the absolute values for Nd(ClO<sub>4</sub>)<sub>3</sub> are at least an order of magnitude greater. Thus, compared to other components of the system, the rate of change of  $B_{\text{NdSO}_4}$  with temperature is low, and we therefore suggest that  $B_{\text{NdSO}_4}$  should be relatively insensitive to changes in temperature. It has to be noted that this assumption leads to a higher (but unknown) level of uncertainty for the results obtained.

We believe that for the present state of knowledge, and given the absence of any experimental data on the behavior of NdSO<sub>4</sub><sup>+</sup> at elevated temperature, the model described above represents the best available approach for calculating activity coefficients for NdSO<sub>4</sub><sup>+</sup>. Fig. 4 compares activity coefficients calculated for a hypothetical solution containing 0.06 mol/L of Nd<sup>3+</sup>, 0.035 mol/L of NdSO<sub>4</sub><sup>+</sup>, 0.015 mol/L of SO<sub>4</sub><sup>2-</sup>, 0.2 mol/L of Na<sup>+</sup>, and 0.2 mol/L of ClO<sub>4</sub><sup>-</sup> using the Pitzer model and the extended Debye–Hückel equation (Helgeson et al., 1981,  $b'_{\text{NaCl}}$  approximation). Both models yield similar values for  $\gamma_{\text{NdSO}_4^+}$  and  $\gamma_{\text{SO}_4^{2-}}$  at elevated temperatures, whereas the values for  $\gamma_{\text{Nd}^{3+}}$  are considerably higher using the extended Debye–Hückel equation.

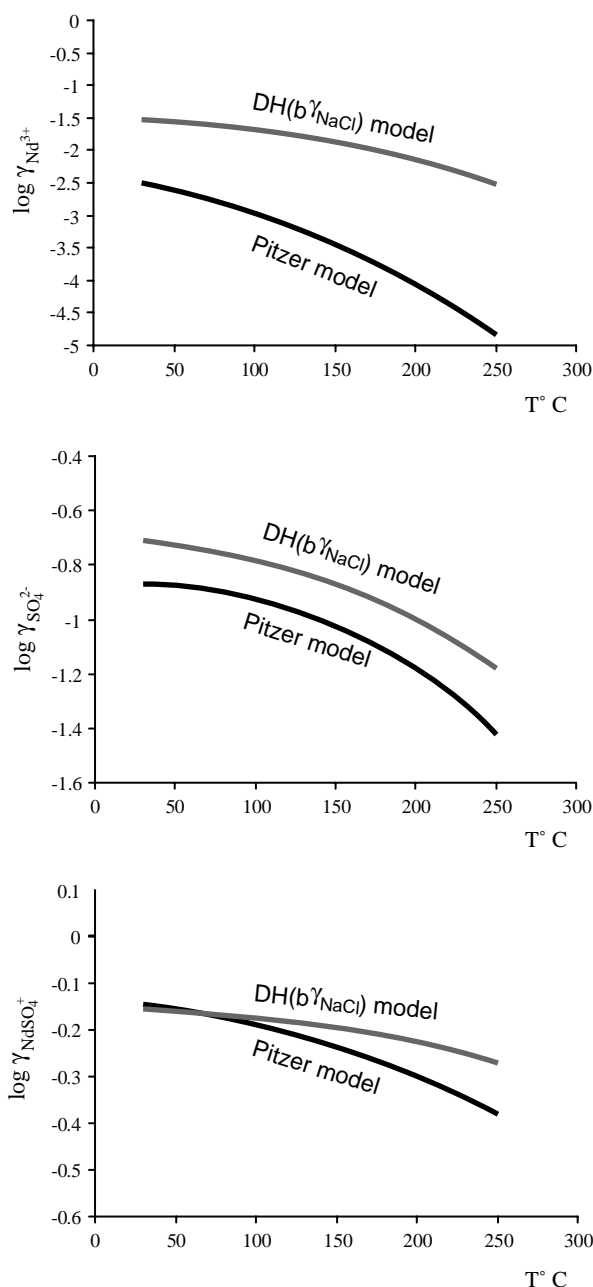
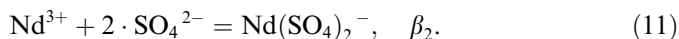


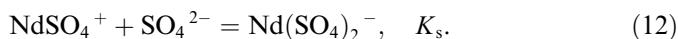
Fig. 4. Results of activity coefficient calculations performed for a hypothetical solution containing 0.06 mol/L of  $\text{Nd}^{3+}$ , 0.035 mol/L of  $\text{NdSO}_4^+$ , 0.015 mol/L of  $\text{SO}_4^{2-}$ , 0.2 mol/L of  $\text{Na}^+$ , and 0.2 mol/L of  $\text{ClO}_4^-$  using the Pitzer model and the extended Debye–Hückel equation (Helgeson et al., 1981,  $b_{\text{NaCl}}^\gamma$  approximation).

#### 4.3. Calculation of the formation constants

Equilibrium constants were calculated for the following complexation reactions:



For the model comprising only  $\text{NdSO}_4^+$  and  $\text{Nd}(\text{SO}_4)_2^-$  (no  $\text{Nd}^{3+}$  present) an equilibrium constant was calculated for the stepwise reaction:



To calculate the equilibrium constants for the reactions Eqs. ((10)–(12)), we used the method described by Suleimov and Seward (2000) and Migdisov and Williams-Jones (2002). The values of the formation constants were refined iteratively from initial guesses via successive minimization of the function:

$$U = \sqrt{\sum_{i=1}^I \left[ \sum_{k=1}^K (A_{ik}^{\text{obs}} - A_{ik}^{\text{calc}})^2 \right]}, \quad (13)$$

where  $i$  is the wavelength,  $I$  is the total number of wavelengths at which measurements were made, and  $K$  is the number of solutions. The variable  $A_{ik}^{\text{calc}}$  is the calculated absorbance, and is a function of the concentrations of the absorbing species and their molar absorbances, whereas  $A_{ik}^{\text{obs}}$  is the absorbance determined experimentally.

The calculations involved several cycles of iteration, which minimized  $U$  in Eq. (13) with respect to the formation constants. Each of the iterations involved calculation of predicted concentrations of species for each of the experimental solutions starting with initial guesses of the formation constants. These concentrations were in turn used to de-convolute the absorbance matrix and to produce optimized values of molar absorbances for each of the experimental wavelengths. Following Hug and Sulzberger (1994) and Boily and Seward (2005), the spectra were de-convoluted using a method that employs singular value decomposition of the absorbance matrix ( $[\text{L}, \text{S}, \text{V}] = \text{SVD}(\text{A})$  produces a diagonal matrix  $\text{S}$ , of the same dimension as  $\text{A}$  with nonnegative diagonal elements in decreasing order, and unitary matrices,  $\text{L}$  and  $\text{V}$ , so that  $\text{A} = \text{L} \cdot \text{S} \cdot \text{V}' + \text{Error}$ ), and calculates the substitute matrix  $\text{R}$  such that  $\text{L} \cdot \text{R}$  is equal to the matrix of concentrations and  $\text{R}' \cdot \text{S} \cdot \text{V}'$  is equal to the matrix of molar absorbances. The molar absorbances of  $\text{Nd}^{3+}$  were not obtained during the iterations, but were introduced directly from experimental data. The final step of each of the iterations involved calculation of the theoretical absorbance matrix (which was done using optimized molar absorbances and concentrations of the species, Eq. (2)) and minimization of the function  $U$  in Eq. (13). The algorithm employed in the minimization was the Nelder–Mead simplex search described by Nelder and Mead (1965), and Dennis and Woods (1987). In Fig. 5, we illustrate molar absorbances for  $\text{NdSO}_4^+$  and  $\text{Nd}(\text{SO}_4)_2^-$  obtained by de-convoluting the spectra at the end of the minimization procedure (MATLAB software; function “fmins”).

The optimization performed for the three-species model gave statistically reliable solutions only for spectra recorded at 30 and 100 °C. At higher temperatures, even minor changes in the initial guesses resulted in significant changes in the results of the optimization, indicating that the analyzed system was over-determined. We therefore concluded that at temperatures above 100 °C, the concentrations of  $\text{Nd}^{3+}$  in the experimental solutions were too low to allow

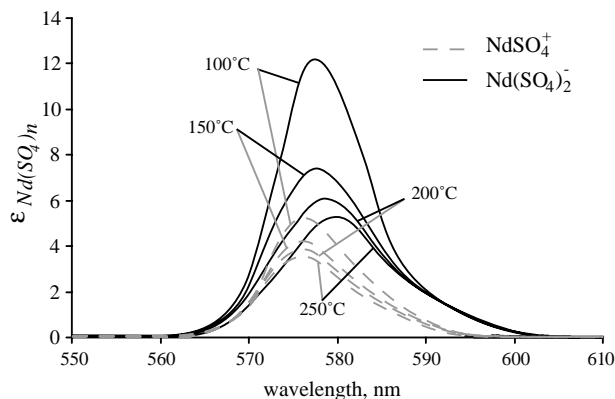


Fig. 5. Molar absorbances for  $\text{NdSO}_4^+$  and  $\text{Nd}(\text{SO}_4)_2^-$  calculated from spectra de-convolution.

Table 4

The logarithms of optimized formation ( $\log \beta$ —see Eqs. (10) and (11)) and stepwise formation constants ( $\log K_s$ ; Eq. (12))

$T$ ( $^\circ\text{C}$ )	$\log K_s$	$\log \beta_1$	$\log \beta_2$
30	1.82*	$3.48 \pm 0.15$	$5.3 \pm 0.14$
100	2.53*	$4.51 \pm 0.16$	$7.04 \pm 0.14$
150	$3.04 \pm 0.15$	—	—
200	$3.51 \pm 0.14$	—	—
250	$4.02 \pm 0.12$	—	—

The values marked by an asterisk were calculated from  $\log \beta_1$  and  $\log \beta_2$ .

it to be reliably identified. Thus, for temperatures above  $100^\circ\text{C}$  we optimized the stepwise constant  $K_s$  Eq. (12), which does not include the ion  $\text{Nd}^{3+}$ . The values of the optimized formation and stepwise constants are listed in Table 4.

To estimate the errors associated with the derivation of the formation constants, we modeled the distribution of the overall error for the treatment of the spectra as function of the formation constants for each of the isotherms investigated. The overall error was calculated using the relationship:

$$\text{Overall error} = 100 \times \sqrt{\frac{\sum_{i=1}^I \left[ \sum_{k=1}^K (A_{ik}^{\text{obs}} - A_{ik}^{\text{calc}})^2 \right]}{\sum_{i=1}^I \left[ \sum_{k=1}^K A_{ik}^{\text{obs}2} \right]}}, \quad (14)$$

where  $I$  is the total number of wavelengths at which measurements were made and  $K$  is the number of solutions. Examples of these distributions for 100 and  $200^\circ\text{C}$  are shown in Figs. 6A and B, respectively, as “profiles” of the overall error versus the values of the guessed formation constants. As can be seen from Fig. 6, the optimized values of the formation constants correspond to the “deepest” depressions in the profiles. On each of the profiles, we show the level, representing the accuracy in the measurement of the spectra. The accuracy was calculated from the values of the tolerance, which were obtained in the rank calculations (see Speciation model) using the relationship:

$$\text{Accuracy} = 100 \times \sqrt{\frac{\sum_{i=1}^I \left[ \sum_{k=1}^K \text{tol}^2 \right]}{\sum_{i=1}^I \left[ \sum_{k=1}^K A_{ik}^{\text{obs}2} \right]}}, \quad (15)$$

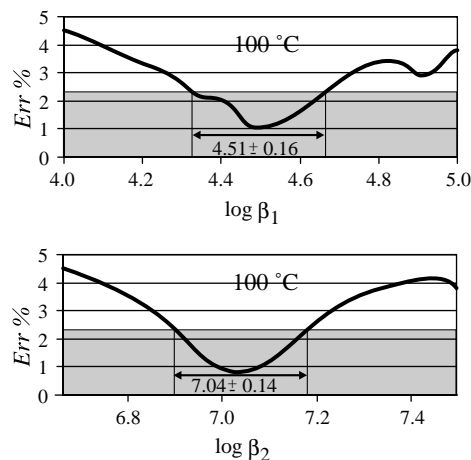


Fig. 6. An example of the distribution of the overall error associated with the treatment of the spectra as a function of the formation constant values. The gray color represents the region for which an accurate derivation of the constant requires a precision higher than that of the experimental method.

where  $\text{tol}$  is the minimum tolerance required for the given speciation model. Projections of this level onto the formation constant axes show the error in the derivation of the corresponding formation constant.

## 5. Discussion

The speciation of REE in sulfate-bearing solutions has been studied extensively at ambient temperature using a variety of techniques including conductimetry, potentiometry, spectrophotometry, solvent extraction, calorimetry, and ion exchange (e.g., Izatt et al., 1969; Spedding and Jaffe, 1954). The results of these studies were reviewed in detail by Wood (1990b), who recommended the values of the formation constant for sulfate complexes at ambient temperature, reported in Tables 5 and 6. The values published in the literature for the logarithm of the first formation constant are in good agreement and vary insignificantly around a value of 3.6. For example, the value of  $\log \beta_1$  calculated from data of Spedding and Jaffe (1954) is 3.63, Izatt et al. (1969) obtained a value of 3.43, Schijf and Byrne (2004) reported a value of 3.6, and Wood (1990b) recommended a value of 3.65. We, thus, consider the value obtained from our experiments (3.48) to be in excellent agreement with the data published in the literature. Similarly, our value for the stability constant of the bi-sulfate complex of neodymium is in very good agreement with the published values. The value proposed by Izatt et al. (1969) for  $\log K_s$  (the stepwise formation constant,  $25^\circ\text{C}$ ) is 1.74, whereas Wood (1990b) recommends a value of 1.5. The value obtained in our study (1.82,  $30^\circ\text{C}$ ) is thus in good agreement with these data and when linearly extrapolated to  $25^\circ\text{C}$  ( $\log K_s$  ( $25^\circ\text{C}$ ) = 1.77) yields a value that is indistinguishable from the value of Izatt et al. (1969).

The only data available for the formation constants of Nd sulfate species at elevated temperatures are the

Table 5  
A comparison of the values of  $\log \beta_1$  obtained in this study with theoretical estimates reported by Wood (1990b) and Haas et al. (1995)

$T$ (°C)	Haas et al. (1995)	Wood (1990)	Our data
25	3.64	3.65	
30			3.48
100	4.53	4.77	4.51
150	5.13	5.62	
200	5.81	6.48	
250	6.63	7.31	

Table 6  
A comparison of the values of  $\log K_s$  obtained in this study with theoretical estimates of Wood (1990b)

$T$ (°C)	Our data	Wood (1990)
25		1.5
30	1.82	
100	2.53	2.27
150	3.04	2.81
200	3.52	3.33
250	4.02	3.83

theoretical estimates made by Wood (1990b) and Haas et al. (1995). At temperatures below 100 °C, these two studies reported similar values for the formation constant of  $\text{NdSO}_4^+$ , but for higher temperatures the estimates diverge and at 250 °C differ by 0.7 logarithmic units. Although our values are closer to those of Haas et al. (1995), the derivative of  $\log \beta_1$  with respect to temperature estimated from our experiments appears to be closer to that predicted by (Wood (1990b), Table 5, Fig. 7). However, we cannot draw these conclusions with any degree of confidence as we determined the values of  $\log \beta_1$  only for temperatures below 150 °C, for which both their estimates are close enough to be statistically indistinguishable. The stepwise constants recommended by Wood (1990b) are very similar to those obtained in our study, and their rates of change with temperature are nearly identical. (Fig. 8, Table 6). Unfortunately, Haas et al. (1995) did not consider bi-sulfate complexes in their speciation model and, thus, do not propose corresponding formation constants. We therefore can-

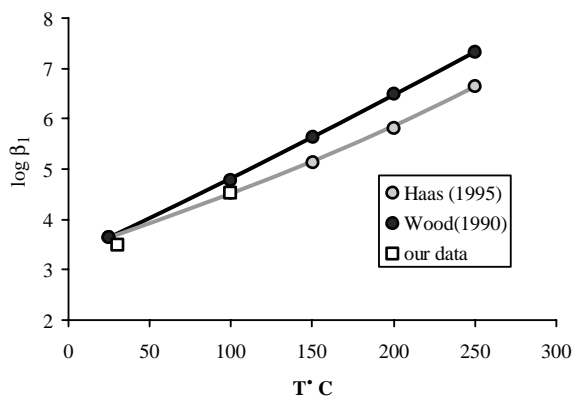


Fig. 7. A comparison of the values of  $\log \beta_1$  obtained in this study with those estimated theoretically by Wood (1990b) and Haas et al. (1995).

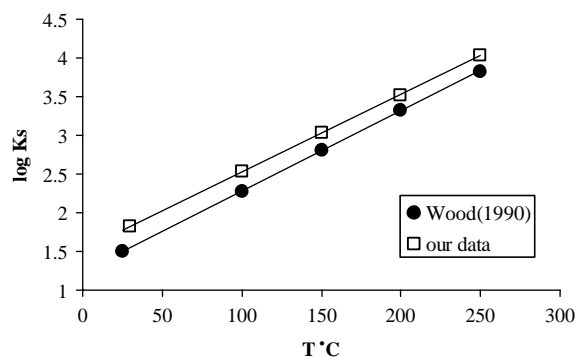


Fig. 8. A comparison of the values of  $\log K_s$  obtained in this study with those estimated theoretically by Wood (1990b).

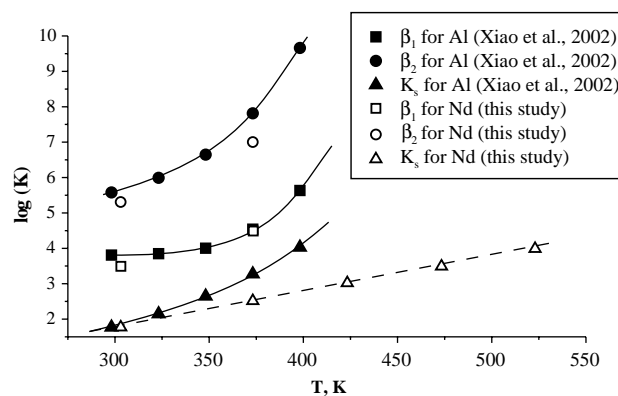


Fig. 9. A comparison of the values of formation constants for Nd-sulfate complexes obtained in this study with those recommended for Al-sulfate complexes.

not compare their data directly with the results of our experiments. However, the close similarity in the temperature dependence of our values for  $K_s$  with those of Wood (1990) suggest that the data of (Haas et al., 1995) would predict a weaker dependency of  $\log K_s$  on temperature than determined by our experiments.

It is worth noting that the formation constants determined in this study are similar to those recommended for Al-SO<sub>4</sub> complexes by Ridley et al. (1999) and Xiao et al. (2002). However, although the values of the formation constants for Al- and Nd-sulfate complexes are nearly identical at low temperatures, the temperature dependencies differ appreciably (Fig. 9); in contrast to Nd the formation constants of Al species vary nonlinearly with respect to temperature. The authors suggested that this nonlinear behavior was a result of a transition from predominantly outer-sphere complexation at low temperature to predominantly inner sphere complexation at high temperature, and supported this conclusion with Raman spectroscopic data. The nearly linear variation of the formation constants of the Nd-sulfate species might therefore indicate that the nature of the complex (inner or outer sphere) did not change over the range of temperatures investigated. Given that the pressure dependency of the formation constant of  $\text{EuSO}_4^+$  at ambient temperature indicates that this species



is an inner sphere complex (Hale and Spedding, 1972) it is likely that Nd-sulfate species interpreted in our study are also inner sphere complexes.

In general, our data support the conclusion of Wood (1990a), that for concentrations of  $\text{SO}_4^{2-}$  typical of natural hydrothermal solutions the dominant species are  $\text{NdSO}_4^+$  and  $\text{Nd}(\text{SO}_4)_2^-$  (in the absence of other ligands), and that the importance of the latter complex increases with increasing temperature. This may have important implications for existing models of REE behavior in natural hydrothermal systems, many of which have been constrained by data of Haas et al. (1995) (e.g., Bach et al., 2003; Lewis et al., 1998). In view of the fact that Haas et al. (1995) did not consider the species  $(\text{Nd}(\text{SO}_4)_2^-)$ , which in our experiments was shown to be important or even dominant over  $\text{NdSO}_4^+$  (e.g., at  $\log C_{\text{SO}_4^{2-}}$  exceeding  $-2.53$ ,  $-3.04$ ,  $-3.52$ , and  $-4.02$  for 100, 150, 200, and 250 °C, respectively) predictions made by these models almost certainly underestimate the solubility of REE in sulfate-rich solutions.

## 6. Conclusions

The experimental data obtained spectrophotometrically in this study confirm the conclusion of Wood (1990) that, for concentrations of  $\text{SO}_4^{2-}$  typical of natural hydrothermal solutions, the dominant species are  $\text{NdSO}_4^+$  and  $\text{Nd}(\text{SO}_4)_2^-$  in the absence of other ligands, and that the latter complex increases in importance with increasing temperature. The values of the formation constants ( $\log \beta_1$ ) obtained in this study for 30 and 100 °C are in excellent agreement with those predicted theoretically by Haas et al. (1995) and Wood (1990b), and the stepwise formation constants ( $K_s$ ) agree reasonably well with the predictions of Wood (1990b).

## Acknowledgments

This research was made possible through grants from NSERC and FQRNT to A.E.W.-J., and the assistance of T. Seward and O. Suleimenov (ETH, Zurich) in the design of the UV-visible cell used in the experiments. O. Suleimenov also provided helpful advise on the de-convolution of spectra. The manuscript benefited from reviews by F. Poitrasson, D. Wesolowski and an anonymous GCA referee.

Associate editor: David J. Wesolowski

## References

- Bach, W., Roberts, S., Vanko, D.A., Binns, R.A., Yeats, C.J., Craddock, P.R., Humphris, S.E., 2003. Controls of fluid chemistry and complexation on rare-earth element contents of anhydrite from the Pacmanus seafloor hydrothermal system, Manus Basin, Papua New Guinea. *Miner. Deposita* **38** (8), 916–935.
- Boily, J., Seward, T., 2005. Palladium(II) chloride complexation: spectrophotometric investigation in aqueous solutions from 5 to 125 °C and theoretical insight into Pd-Cl and Pd-OH<sub>2</sub> interactions. *Geochim. Cosmochim. Acta* **69**, 3773–3789.
- Buhn, B., Rankin, A.H., 1999. Composition of natural, volatile-rich Na-Ca-REE-Sr carbonatitic fluids trapped in fluid inclusions. *Geochim. Cosmochim. Acta* **63** (22), 3781–3797.
- Carnall, W.T., 1979. The absorption and fluorescence spectra of rare earth ions in solution. *Handb. Phys. Chem. Rare Earths* **3**, 171–208.
- Cetiner, Z.S., Wood, S.A., Gammons, C.H., 2005. The aqueous geochemistry of the rare earth elements. Part XIV. The solubility of rare earth element phosphates from 23 to 150 °C. *Chem. Geol.* **217** (1–2), 147–169.
- Dennis, J.E., Jr., Woods, D.J., 1987. In: Wouk, A. (Ed.), *New Computing Environments: Microcomputers in Large-Scale Computing*. SIAM, pp. 116–122.
- Dongarra, J.J., Bunch, J.R., Moler, C.B., Stewart, G.W., 1979. *LINPACK Users' Guide*, SIAM, Philadelphia.
- Gammons, C.H., Wood, S.A., Williams-Jones, A.E., 1996. The aqueous geochemistry of the rare earth elements and yttrium: VI. Stability of neodymium chloride complexes from 25 to 300 °C. *Geochim. Cosmochim. Acta* **60** (23), 4615–4630.
- Gammons, C.H., Wood, S.A., Li, Y., 2002. Complexation of the rare earth elements with aqueous chloride at 200 °C and 300 °C and saturated water vapor pressure. Special Publication—The Geochemical Society, (Water-Rock Interactions, Ore Deposits, and Environmental Geochemistry), 191–207.
- Haas, J.R., Shock, E.L., Sassani, D.C., 1995. Rare earth elements in hydrothermal systems: estimates of standard partial molal thermodynamic properties of aqueous complexes of the rare earth elements at high pressures and temperatures. *Geochim. Cosmochim. Acta* **59** (21), 4329–4350.
- Hale, C.F., Spedding, F.H., 1972. Effect of high pressure on the formation of aqueous  $\text{EuSO}_4^+$  at 25°. *J. Phys. Chem.* **76**, 2925–2929.
- Harvie, C.E., Weare, J.H., 1980. The prediction of mineral solubilities in natural waters: the Na-K-Mg-Ca-Sod-Cl-H<sub>2</sub>O system from zero to high concentration at 25 °C. *Geochim. Cosmochim. Acta* **44**, 981–997.
- Helgeson, H.C., Kirkham, D.H., Flowers, G.C., 1981. Theoretical prediction of the thermodynamic behavior of aqueous electrolytes at high pressures and temperatures: IV. Calculation of activity coefficients, osmotic coefficients, and apparent molal and standard and relative partial molal properties to 600 °C and 5 kb. *Am. J. Sci.* **281** (10), 1249–1516.
- Hug, S.J., Sulzberger, B., 1994. In situ fourier transform infrared spectroscopic evidence for the formation of several different surface complexes of oxalate on TiO<sub>2</sub> in the aqueous phase. *Langmuir* **10**, 3587–3597.
- Izatt, R.M., Eatough, D., Christensen, J.J., Bartholomew, C.H., 1969. Calorimetrically determined  $\log K$ ,  $H^\circ$ , and  $S^\circ$  values for the interaction of sulphate ion with several bi- and ter-valent metal ions. *J. Chem. Soc. London*, 47–53.
- Kotzian, M., Fox, T., Roesch, N., 1995. Calculation of electronic spectra of hydrated Ln(III) ions within the INDO/S-CI approach. *J. Phys. Chem.* **99** (2), 600–605.
- Lakshman, S.V.J., Buddhudu, S., 1982. Optical absorption spectra of neodymium sulfate octahydrate ( $\text{Nd}_2(\text{SO}_4)_3 \cdot 8\text{H}_2\text{O}$ ) complexes in solution. *J. Quant. Spectrosc. RA* **27** (5), 531–540.
- Lewis, A.J., Komninou, A., Yardley, B.W.D., Palmer, M.R., 1998. Rare earth element speciation in geothermal fluids from Yellowstone National Park, Wyoming, USA. *Geochim. Cosmochim. Acta* **62** (4), 657–663.
- MacLean, W.H., 1988. Rare earth mobility at constant inter REE ratios in the alteration zone at the Phelps Dodge massive sulfide deposit, Mattagami, Quebec. *Miner. Deposita* **23**, 231–238.
- Migdisov, Art.A., Williams-Jones, A.E., 2002. A spectrophotometric study of neodymium(III) complexation in chloride solutions. *Geochim. Cosmochim. Acta* **66** (24), 4311–4323.
- Millero, F.J., 1992. Stability constants for the formation of rare earth inorganic complexes as a function of ionic strength. *Geochim. Cosmochim. Acta* **56** (8), 3123–3132.
- Nelder, J.A., Mead, R., 1965. A simplex method for function minimization. *Comput. J.* **7**, 308–313.

- Oelkers, E.H., Helgeson, H.C., 1990. Triple-ion anions and polynuclear complexing in supercritical electrolyte solutions. *Geochim. Cosmochim. Acta* **54** (3), 727–738.
- Olivo, G.R., Williams-Jones, A.E., 1999. Hydrothermal REE-rich eudialyte from the Pilanesberg Complex, South Africa. *Can. Mineral.* **37** (3), 653–663.
- Pitzer, K.S., 1991. Ion interaction approach: theory and data correlation. In: Pitzer, K.S. (Ed.), *Activity Coefficients in Electrolyte Solutions*, second ed. CRC Press, Boca Raton, FL, pp. 75–153.
- Pitzer, K.S., Kim, J.J., 1974. Thermodynamics of electrolytes. IV. Activity and osmotic coefficients for mixed electrolytes. *J. Am. Chem. Soc.* **96**, 5701–5707.
- Pokrovskii, V.A., Helgeson, H.C., 1995. Thermodynamic properties of aqueous species and the solubilities of minerals at high pressures and temperatures: the system  $\text{Al}_2\text{O}_3\text{-H}_2\text{O-NaCl}$ . *Am. J. Sci.* **295** (10), 1255–1342.
- Pokrovskii, V.A., Helgeson, H.C., 1997a. Calculation of the standard partial molal thermodynamic properties of  $\text{KCl}^\circ$  and activity coefficients of aqueous  $\text{KCl}$  at temperatures and pressures to 1000 °C and 5 kbar. *Geochim. Cosmochim. Acta* **61** (11), 2175–2183.
- Pokrovskii, V.A., Helgeson, H.C., 1997b. Thermodynamic properties of aq. species and the solubilities of minerals at high pressures and temperatures: the system  $\text{Al}_2\text{O}_3\text{-H}_2\text{O-KOH}$ . *Chem. Geol.* **137** (3–4), 221–242.
- Ridley, M.K., Wesolowski, D.J., Palmer, D.A., Kettler, R.M., 1999. Association quotients of aluminum sulphate complexes in NaCl media from 50 to 125 °C: results of a potentiometric and solubility study. *Geochim. Cosmochim. Acta* **63**, 459–472.
- Robie, R.A., Hemingway, B.S., 1995. Thermodynamic properties of minerals and related substances at 298.15 K and 1 Bar (105 Pascals) pressure and at higher temperatures. *US Geological Survey Bulletin* **2131**, 461.
- Salvi, S., Williams-Jones, A.E., 1990. The role of hydrothermal processes in the granite-hosted zirconium, yttrium, REE deposit at Strange Lake, Quebec/Labrador: evidence from fluid inclusions. *Geochim. Cosmochim. Acta* **54** (9), 2403–2418.
- Schandl, E.S., Gorton, M.P., 1991. Post ore mobilization of rare earth elements at Kidd Creek and other Archean massive sulfide deposits. *Econ. Geol.* **86**, 1546–1553.
- Schijf, J., Byrne, R.H., 2004. Determination of  $\text{SO}_4\beta_1$  for yttrium and the rare earth elements at  $I = 0.66$  m and  $t = 25$  °C—implications for YREE solution speciation in sulfate-rich waters. *Geochim. Cosmochim. Acta* **68**, 2825–2837.
- Silvester, L.F., Pitzer, K.S., 1978. Thermodynamics of electrolytes. X. Enthalpy and the effect of temperature on the activity coefficients. *J. Solution Chem.* **7** (5), 327–337.
- Smith, M.P., Henderson, P., 2000. Preliminary fluid inclusion constraints on fluid evolution in the Bayan Obo Fe-REE-Nb deposit, Inner Mongolia, China. *Econ. Geol.* **95** (7), 1371–1388.
- Spedding, F.H., Jaffe, S., 1954. Conductances, solubilities and ionization constants of some rare earth sulfates in aqueous solutions at 25°. *J. Am. Chem. Soc.* **76**, 882–884.
- Stepanchikova, S.A., Kolonin, G.R., 1999. Spectrophotometric study of complexation of neodymium in chloride solutions at temperatures up to 250 °C. *Zh. Neorg. Khim.* **44** (10), 1744–1751.
- Suleimenov, O.M., Seward, T.M., 2000. Spectrophotometric measurements of metal complex formation at high temperatures: the stability of Mn(II) chloride species. *Chem. Geol.* **167** (1–2), 177–192.
- Weare, J.H., 1989. Models of mineral solubility in concentrated brines with application to field observations. *Rev. Mineral.* **17**, 143–171.
- Williams-Jones, A.E., Samson, I.M., Olivo, G.R., 2000. The genesis of hydrothermal fluorite-REE deposits in the Gallinas Mountains, New Mexico. *Econ. Geol.* **95** (2), 327–341.
- Wood, S.A., 1990a. The aqueous geochemistry of the rare-earth elements [REE] and yttrium. 1. Review of available low-temperature data for inorganic complexes and the inorganic REE speciation of natural waters. *Chem. Geol.* **82** (1–2), 159–186.
- Wood, S.A., 1990b. The aqueous geochemistry of the rare-earth elements and yttrium. 2. Theoretical predictions of speciation in hydrothermal solutions to 350 °C at saturation water vapor pressure. *Chem. Geol.* **88** (1–2), 99–125.
- Wood, S.A., Wesolowski, D.J., Palmer, D.A., 2000. The aqueous geochemistry of the rare earth elements IX. A potentiometric study of  $\text{Nd}^{3+}$  complexation with acetate in 0.1 molal NaCl solution from 25 °C to 225 °C. *Chem. Geol.* **167** (1–2), 231–253.
- Wood, S.A., 1990. The aqueous geochemistry of the rare-earth elements [REE] and yttrium. 1. Review of available low-temperature data for inorganic complexes and the inorganic REE speciation of natural waters. *Chem. Geol.* **82** (1–2), 159–186.
- Wood, S.A., Palmer, D.A., Wesolowski, D.J., Benezeth, P., 2002. The aqueous geochemistry of the rare earth elements and yttrium. Part XI. The solubility of  $\text{Nd}(\text{OH})_3$  and hydrolysis of  $\text{Nd}^{3+}$  from 30 to 290 °C at saturated water vapor pressure with in-situ pH measurement. Special Publication—The Geochemical Society, (Water-Rock Interactions, Ore Deposits, and Environmental Geochemistry), 229–256.
- Xiao, C., Wesolowski, D.J., Palmer, D.A., 2002. Formation quotients of aluminum sulfate complexes in  $\text{NaCF}_3\text{SO}_3$  media at 10, 25, and 50 °C from potentiometric titrations using a mercury/mercurous sulfate electrode concentration cell. *Environ. Sci. Technol.* **36**, 166–173.